J Appl Electrochem (2008) 38:321–327
DOI 10.1007/s10800-007-9441-y

ORIGINAL PAPER

# Use of experimental design to empirically model atmospheric corrosion of galvanised steel

**Emilie Dubuisson · Sabine Szunerits · Jean-Pierre Caire · Philippe Lavie · Sarah Cordier**

Received: 2 January 2007 / Revised: 26 October 2007 / Accepted: 30 October 2007 / Published online: 16 November 2007


**Abstract** Electrochemical impedance spectroscopy in 500–1100 μm large liquid droplets containing chloride and sulphate ions has been used to investigate the local corrosion rate of galvanised steel. The objective was the empirical modelling of the corrosion rate as a function of temperature, electrolyte thickness, and chloride and sulphate concentrations. The first experiments showed that the corrosion time was one of the critical parameters; it was then included in the investigation. An empirical numerical model was obtained for steel and galvanised steel. The statistical model highlighted the respective importance of the five parameters on atmospheric corrosion and gave qualitative results in accordance with the literature. The statistical study also suggested that the corrosion potential was easier to model than corrosion currents.

**Key words** Experimental design · Atmospheric corrosion · Galvanised steel

## 1 Introduction

The knowledge of the corrosion rate of galvanised steel under thin layer configuration is of great industrial importance. Numerical modelling of corrosion phenomena is thus particularly interesting as it allows forecasting the life time of vehicles and helping the development of better bodywork designs [1]. We recently described an original experimental method to study the local corrosion rate of galvanised steel [2]. Localised measurements were achieved through the controlled deposition of an electrolyte droplet onto the sample, where reference and counter electrodes were incorporated forming an electrochemical micro cell [3].

While numerous electrochemical studies can be found in the literature concerning the individual role of each parameter, (e.g. temperature, ionic concentrations, electrolyte thickness) there is until now no numerical model able to forecast the corrosion of steel and galvanised steel as a function of these parameters. We show here the development of an empirical model for the corrosion rate of steel and galvanised steel including the main parameters encountered in the car life cycle, namely temperature, thickness of the electrolyte layer, chloride and sulphate concentrations.

The response surface methodology (RSM) [4] based on the design of experiments (DOE) [5] has been rarely used in the field of electrochemistry [6] and corrosion [7–10]. Here RSM was used in conjunction with the droplet measurement technique [2, 3] in an electrochemical micro cell to obtain the empirical model of interest.

## 2 Assumptions and definition of the experimental domain

The corrosion phenomena encountered include galvanic corrosion, pitting, corrosion under coating layer, etc. which are all interlinked in the case considered. Due to the complexity of such interrelated phenomena an empirical model obtained by the design of experiments methodology is the best way to obtain quantitative responses as a function of all the parameters.

E. Dubuisson · S. Szunerits · J.-P. Caire (✉)
LEPMI, ENSEEG, UMR 5631 INPG – CNRS, 1130 Rue de la Piscine, 38402 Saint-Martin d'Heres, France
e-mail: jean-pierre.caire@lepmi.inpg.fr

P. Lavie · S. Cordier
PSA Peugeot Citroën, DITV/PMXP/MXP/PEI, route de Gisy, 78 943 Velizy-Villacoublay, France

A literature survey showed that the main influential variable parameters of the corrosion rate of galvanised steel in the presence of chloride and sulphate ions are: temperature, thickness of the electrolyte layer, pH and chloride and sulphate concentrations [1]. In addition, several simplifying initial assumptions were included. The metal surfaces were considered to be in an initial state without surface treatment such as phosphatising, cataphoresis or paint coating. The galvanic coupling between the sacrificial zinc deposit and the steel substrate is not modelled here. All the runs were made using samples from the same industrial sheet in order to avoid a so-called block effect [5].

The corrosion study under thin electrolyte layers was based on electrochemical impedance measurements in aqueous micro droplets. Due to oxygen diffusion the height of the droplet strongly influences the corrosion rate of the underlying metal. Determination of the equivalent thickness, h, defined as the cylindrical film having the same volume and diameter as the droplet, was thus required (see Fig. 1). The average height, h, of the electrolyte drop was obtained from optical measurements of the height, H, and diameter, d, of the drop. A simple calculus shows that h is related to H and d by the relation:

$$h = H\left[\frac{1}{2} + \frac{2}{3}\left(\frac{H}{d}\right)^2\right] \quad (1)$$

This equivalence is not fully justified since the diffusion of oxygen, the driving force of corrosion, is quite different in a drop and a film.

The limiting values of each parameter were carefully chosen taking into consideration the experimental limitations of the micro droplet experiment. From an ideal corrosion point of view, it would have been necessary to use a lower limit close to 100 μm for the electrolyte layer thickness h. The H = 500 μm (h = 274 μm) value used here was chosen as a result of the preliminary replicate tests which showed that the dispersion was far too large for thinner layers with the EIS in droplet method [1]. The limiting values for each variable are presented in Table 1.

The high and low levels for each variable are presented in Table 1. The chloride and sulphate concentrations

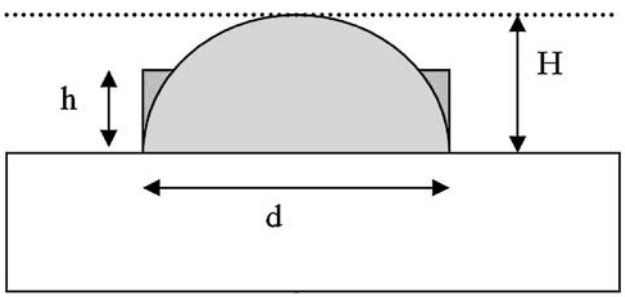


**Fig. 1** Equivalent thickness h of a droplet of height H and diameter d

**Table 1** Limiting values of the parameters studied

| Parameter | Low limit | High limit |
|---|---|---|
| Temperature (°C) | 10 | 50 |
| Electrolyte droplet thickness (μm) | H = 500 | H = 1100 |
| | h = 274 | h = 578 |
| Chloride concentration (mg $L^{-1}$) | 30 | 50,000 |
| Sulphate concentration (mol $L^{-1}$) | 5 $10^{-5}$ | $10^{-2}$ |

**Table 2** Design variables and their low and high limits

| Parameter | Variable | Low limit | High limit |
|---|---|---|---|
| Temperature (°C) | T | 10 | 50 |
| Electrolyte layer thickness (μm) | H | 500 | 1000 |
| log(Chloride concentration) | Log Cl | −1.48 | +1.69 |
| log(Sulphate concentration) | Log $SO_4$ | −4.3 | −2.0 |
| Time (min) | Time | 18 | 20 |

spanned three decades and a logarithmic transformation of the concentrations was required to obtain a better precision on the final results. The theoretical bases and the advantages of such a transform can be found in Box et al. [5]. The corrosion time was added as an important parameter due to a time delay in recording the experimental data. The final choice of the five design variables, with their design variable name, are as follows (Table 2).

## 3 Studied response

The corrosion current density $i_{corr}$ (A $cm^{-2}$) was the only response taken into account in the DOE. It was obtained from the polarisation resistance, *R*p, measured by electrochemical impedance spectroscopy (EIS) and using 6 × $10^{-3}$ V for K in the Stern and Geary equation [11]:

$$i_{corr} = \frac{K}{Rp} \quad (2)$$

## 4 Design of the experiments

The design of experiments was made with ECHIP6 code [12] for a Response surface methodology (RSM) [4]. A so called "composite centred in a cube" design (CCI) was chosen from ECHIP6 since it offered a good compromise in terms of experimental cost and efficiency. The 27 different experimental runs of the CCI design seen in Table 3 were randomized. The central point (denoted 27) was replicated 5 times and was used to estimate the experimental variance. Seven extra experimental runs (numbered 1000–1006) situated inside the experimental ~domain were used as check points to estimate the quality of prediction of the empirical model.

**Table 3** Design of experiments

| Run | T (°C) | H (μm) | LogCl (mg $L^{-1}$) | Log$SO_4$ (mg $L^{-1}$) | Time (min) |
|---|---|---|---|---|---|
| 15 | 49 | 1100.000 | 1.7000 | −4.3000 | 22.22 |
| 9 | 31 | 800.000 | 0.1000 | −3.1500 | 18.6 |
| 23 | 10.000 | 1100.000 | 1.7000 | −4.3000 | 19.5 |
| 27 | 30.000 | 800.000 | 0.1000 | −3.1500 | 20.08 |
| 6 | 30.000 | 800.000 | 1.7000 | −3.1500 | 20.05 |
| 17 | 10.000 | 1100.000 | −1.5000 | −4.3000 | 21.3 |
| 13 | 49 | 1100.000 | −1.5000 | −2.0000 | 22 |
| 3 | 30.000 | 500.000 | 0.1000 | −3.1500 | 20.2 |
| 27 | 31 | 800.000 | 0.1000 | −3.1500 | 19.76 |
| 5 | 31 | 800.000 | −1.5000 | −3.1500 | 19.95 |
| 14 | 10.000 | 500.000 | −1.5000 | −2.0000 | 22.28 |
| 4 | 30.000 | 1100.000 | 0.1000 | −3.1500 | 20.66 |
| 22 | 49 | 500.000 | −1.5000 | −2.0000 | 18.12 |
| 8 | 32 | 800.000 | 0.1000 | −2.0000 | 20.32 |
| 18 | 50.000 | 500.000 | −1.5000 | −4.3000 | 22.4 |
| 16 | 10.000 | 500.000 | 1.7000 | −4.3000 | 21.3 |
| 1 | 10.000 | 800.000 | 0.1000 | −3.1500 | 20.28 |
| 12 | 49 | 500.000 | 1.7000 | −2.0000 | 22.1 |
| 7 | 33 | 800.000 | 0.1000 | −4.3000 | 20.25 |
| 24 | 49 | 500.000 | 1.7000 | −4.3000 | 19.02 |
| 11 | 12 | 1100.000 | 1.7000 | −2.0000 | 21.58 |
| 25 | 48 | 1100.000 | −1.5000 | −4.3000 | 18 |
| 2 | 50.000 | 800.000 | 0.1000 | −3.1500 | 19.95 |
| 27 | 30.000 | 800.000 | 0.1000 | −3.1500 | 20.15 |
| 20 | 10.000 | 500.000 | 1.7000 | −2.0000 | 18.23 |
| 10 | 30.000 | 800.000 | 0.1000 | −3.1500 | 21.63 |
| 19 | 49 | 1100.000 | 1.7000 | −2.0000 | 18.07 |
| 21 | 10.000 | 1100.000 | −1.5000 | −2.0000 | 18 |
| 27 | 30.000 | 800.000 | 0.1000 | −3.1500 | 20.05 |
| 27 | 30.000 | 800.000 | 0.1000 | −3.1500 | 20.13 |
| 26 | 10.000 | 500.000 | −1.5000 | −4.3000 | 18.43 |
| 1000 | 35 | 500 | 1 | −4 | 18.2 |
| 1001 | 35 | 500 | 1 | −4 | 18.12 |
| 1002 | 40 | 800 | 0 | −3 | 18.05 |
| 1003 | 40 | 800 | 0 | −3 | 18 |
| 1004 | 40 | 800 | 0 | −3 | 18.77 |
| 1005 | 20 | 1100 | −1 | −2.5 | 18.08 |
| 1006 | 20 | 1100 | −14 | −2.5 | 18.017 |

For practical reasons the experimental time values appearing in Table 3 replace the optimal times given in the original CCI design (18, 20, 22 min).

## 5 Empirical model for the corrosion current density (galvanised steel)

The empirical model expressed in centred variables with ECHIP6 for $i_{corr}$ is:

$$\begin{aligned} i_{corr} = & -z_0 - z_1(Ep - 800) + z_2(\log Cl - 0.1) \\ & -z_3(\log Cl - 0.1) \cdot (\log SO_4 + 3.15) \\ & -z_5(Ep - 800)^2 + z_6(\log Cl - 0.1)^2 \\ & +z_7(temps - 20)^2 \end{aligned} \quad (3)$$

This model was obtained after the refining process consisting in the elimination of the non-significant terms. The true coefficients are replaced hereafter by $z_i$ dummy terms for confidentiality. Though complex, the model is satisfactory for the corrosion current density. We obtained

non-adjusted and adjusted correlation coefficients of $R^2 = 0.965$ and $R^2_{adj} = 0.952$, respectively, using 22 degrees of freedom. Both values are larger than the usual 0.8 value generally required for prediction. However, a "Lack of Fit" warning was issued by the code. There are two main reasons for such behaviour: (i) the model required a transformation of response; (ii) the replicate error was too large.

The analysis of variance (ANOVA) and the study of residuals showed that the residuals were not normal suggesting a logarithmic transformation [4]. We therefore concluded that the model did not fit well. It appeared that the logarithmic transformation gave the better results.

### 5.1 Modelling ln ($i_{corr}$) in comparison with the model of $i_{corr}$ (galvanised steel)

The ln ($i_{corr}$) model expressed in centred variables is:

$$\begin{aligned}\ln(i_{corr}) = &-z_0 - z_1(Ep - 800) + z_2(\log Cl - 0.1)\\ &-z_3(\log Cl - 0.1)\cdot(\log SO_4 + 3.15)\\ &-z_5(Ep - 800)^2 + z_6(\log Cl - 0.1)^2\\ &+z_7(temps - 20)^2\end{aligned} \quad (4)$$

The statistical tests all passed and the residuals were normal. It appeared that this empirical model fitted well the experimental data and could be used for prediction.

In the Pareto effects graph of Fig. 2, the influential terms of the model are ordered according to the magnitude of the dimensionless effects (the segments represent their 95% confidence interval). It may be concluded that:

- LogCl is the most influential variable acting with linear and quadratic effects (terms 3 and 18 of Fig. 2). Moreover it interacts with the concentration of sulphate (term 13 of Fig. 2). The larger the chloride concentration, the larger the corrosion current.
- the corrosion current increases in a quadratic way with chloride concentration when the droplet thickness increases.
- corrosion time, between 18 and 22 min, is one of the most influential variables.

All these conclusions perfectly match literature results [14, 15]. The interaction between sulphate and chloride

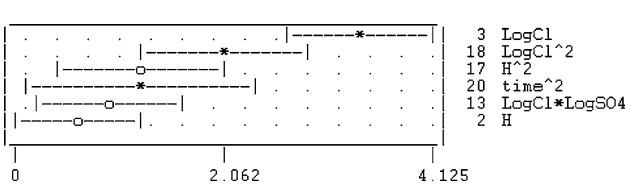


**Fig. 2** Pareto effect graph of log($i_{corr}$) for galvanised steel (Screen copy from ECHIP6)

**Table 4** Comparison of experimental and predicted values

| Run | Ln ($i_{corr}$) (mA cm$^{-2}$) | | 95% confidence intervals |
|---|---|---|---|
| | Experimental values | Predicted values | Low and high limits |
| 1000 | −8.31 | −9.65 | (−11.18, −8.12) |
| 1001 | −8.61 | −9.58 | (−11.13, −8.04) |
| 1002 | −11.25 | −10.56 | (−12.14, −8.99) |
| 1003 | −10.59 | −10.524 | (−12.11, −8.93) |
| 1004 | −12.12 | −11.06 | (−12.49, −9.62) |
| 1005 | −11.69 | −12.08 | (−13.59, −10.58) |
| 1006 | −11.35 | −12.03 | (−13.54, −10.52) |

ions is not surprising. The main advantage of design of experiments is in the quantification of these effects and the possibility of rapid and precise prediction of any new situation (in the experimental domain) thanks to the numerical model.

Table 4 compares the experimental and predicted values for the extra checkpoints runs. As expected, all the predicted values fall inside the 95% confidence limits. The coherence of results is evident but the confidence intervals are too large. To improve the prediction quality, i.e. to reduce the interval between low and high limits of prediction, a multiple replication of the same design would have to be performed.

Figure 3-left gives the 2D contour plots as a function of the two main influential variables LogCl and H for given values of T, Log$SO_4$ and time. Replacing variable H by time transforms the shape of the contour plots from saddle to hillock.

The so called "convex hull" of Fig. 3-right is a polygon passing by the experimental points [12]. This polygon represents the projection on the plane (LogCl, H) of the five dimension convex domain where the model can be used. For a CCI design, this polygon is a square. As seen in Fig. 3-right, the "convex hull" is not a perfect square in the last case. This is due to the experimental duration which was not perfectly controlled in the experimental set up. These 2D contour plots show that there are infinite sets of [H, LogCl] combinations that give the same corrosion rate. For example the −12.0 value of variable Log $i_{corr}$ can be obtained on two different hyperboles for given values of T, Log$SO_4$ and time. In this case the variable LogCl must be chosen in the interval [−1.5, 0.5]. The figure also shows that the larger corrosion values are obtained for large LogCl and medium values of H. It can be seen that in the domain appearing here, Log $i_{corr}$ is defined in the interval [−8.0, −13.0] and $i_{corr}$ varies thus by five decades. This explains *a posteriori* the necessity of the logarithmic transformation. It also confirms the well known possibility of making accelerated corrosion tests. Such 2D contour

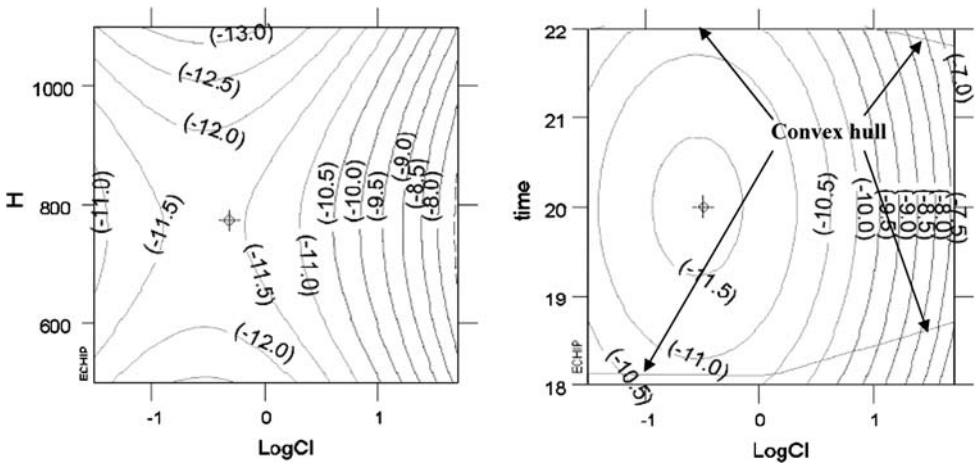


**Fig. 3** Two different 2D contour plots of $\ln(i_{corr})$ for galvanised steel

plots give the best way to boost the corrosion phenomena by numerical optimization of the response, as done here.

### 5.2 Physical interpretation of the empirical model results

Response surface methodology has shown that the $\ln(i_{corr})$ model was the best. A physical interpretation of this result was attempted. The overpotential $\eta$ associated with any electrochemical reaction is:

$$\eta = E - E_{th} \tag{5}$$

where E is the electrochemical potential. The current density, i, is related to the over potential $\eta$ by the simplified Butler–Volmer relation related to charge transfer control [13]:

$$i = i_o\left[e^{(a_{ox}\frac{nF}{RT}h)} - e^{(\alpha_{red}\frac{nF}{RT}\eta)}\right] \tag{6}$$

where $i_o$ is the exchange current density and $\alpha$ the symmetry factor or transfer coefficient. For overpotentials larger than 80 mV this relation can be replaced by the Tafel equation:

$$\log(i) = f(\eta) \tag{7}$$

For large anodic over potential, the Tafel equation is:

$$i = i_o\left[e^{(\alpha_{ox}\frac{nF}{RT}\eta)}\right] \tag{8}$$

The relation can be transformed to:

$$\ln\left(\frac{i}{i_o}\right) = \alpha_{ox}\frac{nF}{RT}\eta \tag{9}$$

using the Nernst equation:

$$\eta = \frac{RT}{nF\alpha_{ox}}\ln\left(\frac{i}{i_o}\right) \tag{10}$$

or

$$\eta = \left(\frac{2.3RT}{F}\right)\frac{1}{\alpha_{ox}n}\log\left(\frac{i}{i_o}\right) \tag{11}$$

If the potential $E$ is equal to the corrosion potential $E_{corr}$, Eq. 9 becomes:

$$\eta_{i_{corr}} = \left(\frac{2.3RT}{F}\right)\frac{1}{\alpha_{ox}n}\log\left(\frac{i_{corr}}{i_o}\right) = \left(\frac{RT}{F}\right)\frac{1}{\alpha_{ox}n}\ln\left(\frac{i_{corr}}{i_o}\right) \tag{12}$$

and finally:

$$\eta_{i_{corr}} = \left(-\frac{RT\ln(i_o)}{\alpha_{ox}nF}\right) + \frac{RT}{\alpha_{ox}nF}\ln(i_{corr}) \tag{13}$$

This relation explains the so called "Lack of fit" found in the statistical tests for the empirical model of $i_{corr}$. Modelling the logarithm of $i_{corr}$ is not simply a transformation made to normalize the residuals as explained in [4]. In fact, such a transformation changes the physical variable and replaces $i_{corr}$ by the overpotential $\eta_{jcorr}$ or the corrosion potential $E_{corr}$. The current density $i_{corr}$ is not the most significant physical variable of this study, but rather the corrosion potential. Due to the use of response surface methodology the true physical variable could be found.

### 5.3 Two examples employing the empirical model

The main advantage of a polynomial model is its ability to give contour plots. Figure 4 presents the dependence of the corrosion current on chloride concentration for electrolyte droplets of 800 μm in height in the presence of sulphuric acid ($7.1 \times 10^{-4}$mol $L^{-1}$) after 20 min of corrosion. The predicted corrosion current increases rapidly for chloride concentration larger than 3 g $L^{-1}$; this is a vigorous accelerating factor of corrosion well described in this model. The variation of corrosion current density with

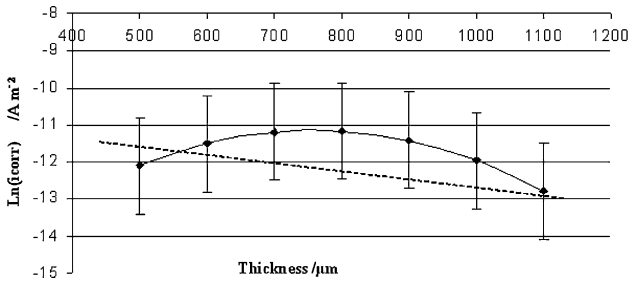


**Fig. 5** Logarithm of corrosion current density as a function of the thickness of the droplet, after 20 min, in the presence of sulphuric acid (7.1 $10^{-4}$ mol $L^{-1}$) and a chloride concentration of 1.58 g $L^{-1}$

droplet thickness, as seen in Fig. 5, is not linear as reported previously [13], in accordance with the polynomial model. From the experimental dispersion, both linear and non-linear models can be considered. In fact the model prediction is probably non-linear since ln($i_{corr}$) is plotted against H instead of h. The curvature could also be related to the passivation of zinc (Fig. 6).

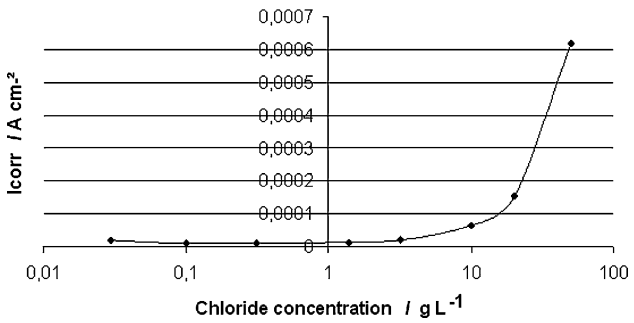


**Fig. 4** Corrosion current density versus chloride concentration for a 800 µm droplet obtained by the empirical model of galvanised steel

## 6 Design of experiments for steel

The same methodology as described above was developed for steel, with the same physical parameters and the same CCI design of experiments to determine the corrosion rate for the case of lack or disappearance of the sacrificial material. The response seen in Fig. 6 was:

$$\log(i_{corr}) = \log_{10}\left(\frac{0.0135}{R_p}\right) \quad (14)$$

The Stern–Geary coefficient K = 0.0135 V was obtained by a method similar to that used for galvanised steel. The refined empirical model is:

$$\begin{aligned}\log(i_{corr}) = &-a_0 + a_1(T-30) - a_2(Ep-800)\\ &+a_3(\log Cl - 0.1) + a_4(t-20)\\ &-a_5(T-30)(\log SO_4 + 3.15)\\ &-a_6(\log Cl - 0.1)(\log SO_4 + 3.15)\\ &+a_7(T-30)^2 + a_8(\log Cl - 0.1)^2\end{aligned} \quad (15)$$

The significant parameters are the temperature-sulphate and chloride-sulphate interaction. All the empirical results match the experiments and the corrosion rate is seven decades larger when the steel is not protected by zinc. From a statistical point of view, compared to the model of galvanized steel, the model is badly defined. This is probably due to the larger corrosion rate values recorded. A better prediction could be obtained by replicating the design several times.

## 7 Limitation of the models

One limitation of the models is related to the lack of precision due to the dispersion of the measurements, while the other is linked to the short experimental durations

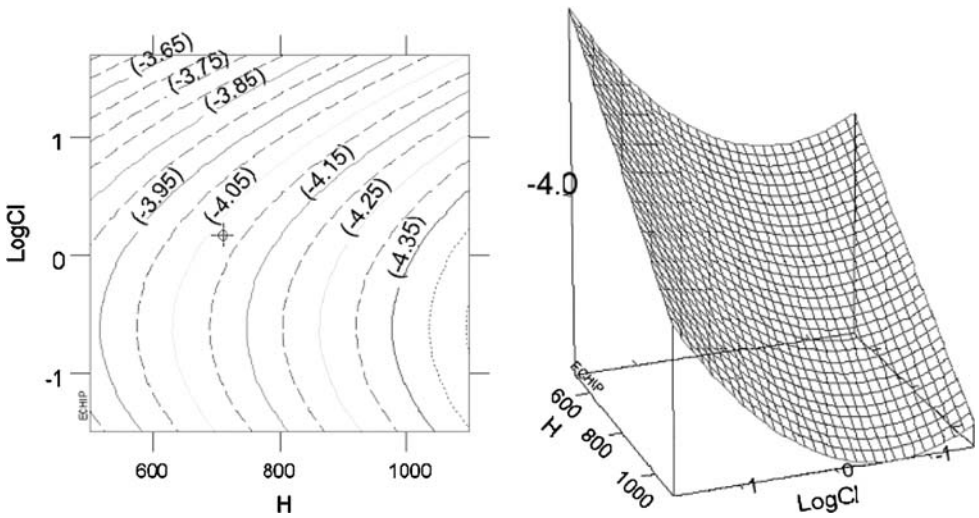


**Fig. 6** 2D contour plots and 3D response surface of log $i_{corr}$ for steel

(18–22 min) used for the RSM. The model can therefore only be used to predict the corrosion rate after 20 min of initiated corrosion, though it is required to simulate a long-term life of the vehicle.

Indeed, for corrosion times as long as 24 h or 48 h under the same corrosion conditions, El-Mahdy and Kim [15] observed a significant attenuation of the corrosion current with time. This effect is due to corrosion products formed at the metal surface. The accumulation of carbonates masks the metal surface and thus limits the access of oxygen to the surface resulting in a decrease in corrosion rate. This is more pronounced for a surface which does not undergo rinsing throughout time. The model does not take into account the attenuation of the corrosion current with time. Including an experimental attenuation factor function taking into consideration the time factor and the presence of corrosion products would be beneficial. This can be done by dropping a liquid droplet on the metal and letting corrosion act until complete evaporation of the drop. The complete process with or without rinsing would be repeated a great number of times during several hours (or days or weeks) to obtain an attenuation factor of the corrosion current as a function of time. Such an experiment is, however, time consuming and costly and was not performed. Nevertheless, for industrial applications the proposed method can be used to determine the empirical corrosion rate of galvanized steel samples having undergone a surface treatment such as phosphatising or organic coating.

## 8 Conclusions

Two empirical models were obtained by use of response surface methodology for the corrosion rate of steel and galvanised steel. The statistical study has shown that the corrosion potential was the appropriate response variable. This conclusion is probably true for any attempt at modelling corrosion rates. Both models are complex quadratic polynomials giving pertinent physical results all depending on the five parameters involved in the study. The importance of the time factor was highlighted. We are currently working on the formulation of an attenuation factor related to the wetting-evaporation cycles and to predict long time corrosion. However, the present numerical models can be already easily included in a larger model that is in progress at PSA.

## References

1. Lavie P (2006) Modélisation de la corrosion et application à la conception automobile, Thesis, INPG, Grenoble
2. Dubuisson E, Lavie P, Dalard F, Caire JP, Szunerits S (2007) Corros Sci 49:910–919
3. Dubuisson E, Lavie P, Dalard F, Caire JP, Szunerits S (2006) Electrochem Commun 8:887–891
4. Box GEP, Draper N (1987) Empirical model-building and response surfaces. Wiley, New-York
5. Box GEP, Hunter WG, Hunter JS (1978) Statistics for experimenters. John Wiley, NY
6. Martinet S, Bouteillon J, Caire JP (1998) J Appl Electrochem 28:819–825
7. Mansfeld F (2005) Corros Sci 47:3178–3186
8. Mansfeld F, Lin SH, Kwiatkowski L (1993) Corros Sci 34(12):2045–2058
9. Ronconi CM, Pereira EC (2001) J Appl Electrochem 31:319–323
10. Vlyssides AG, Arapoglou DG, Israilides CJ, Barampouti EMP, Mai ST (2004) J Appl Electrochem 34:1265–1269
11. Stern M, Geary AL (1957) J Electrochem Soc 104:56
12. ECHIP Version 6.1.2, 724, Yorklyn Road, Hockessin, DE, 19707, USA
13. Diard JP, Le Gorrec B, Montella C (1999) Cinétique électrochimique. Hermann, Paris
14. Qu Q, Yan CI, Wan Y, Cao C (2002) Corros Sci 44:2789
15. El-Mahdy GA, Kim KB (2005) Corrosion 61(5):420